water

MDPI

Article

Construction of Novel Electro-Fenton Systems by Magnetically Decorating Zero-Valent Iron onto RuO_2-IrO_2/Ti Electrode for Highly Efficient Pharmaceutical Wastewater Treatment

Miao Deng [1,2], Keming Wu [1], Tao Yang [3], Deyou Yu [2,4,*], Gaojie Liu [5], Shuai Gong [1], Dongni Sun [1] and Michal Petru [3]

1 State Environment Protection Key Laboratory of Mineral Metallurgical Resources Utilization and Pollution Control, Wuhan University of Science and Technology, Wuhan 430081, China; es_muss_sein_@sohu.com (M.D.); wukeming@wust.edu.cn (K.W.); g2051405195@163.com (S.G.); dongnisun@foxmail.com (D.S.)
2 Key Laboratory of Advanced Textile Materials and Manufacturing Technology, Ministry of Education, College of Textile Science and Engineering, Zhejiang Sci-Tech University, Hangzhou 310018, China
3 Institute for Nanomaterials, Advanced Technologies and Innovation, Technical University of Liberec, 461 17 Liberec, Czech Republic; tao.yang@tul.cz (T.Y.); michal.petru@tul.cz (M.P.)
4 Tongxiang Research Institute, Zhejiang Sci-Tech University, Tongxiang 345000, China
5 The Second Construction Co., Lid of China Construction Third Engineering Bureau, Wuhan 430073, China; 15670536260@sohu.com
* Correspondence: yudeyou92@zstu.edu.cn

check for updates

Citation: Deng, M.; Wu, K.; Yang, T.; Yu, D.; Liu, G.; Gong, S.; Sun, D.; Petru, M. Construction of Novel Electro-Fenton Systems by Magnetically Decorating Zero-Valent Iron onto RuO_2-IrO_2/Ti Electrode for Highly Efficient Pharmaceutical Wastewater Treatment. *Water* **2022**, *14*, 1044. https://doi.org/10.3390/w14071044

Academic Editor: Alexandre T. Paulino

Received: 10 February 2022
Accepted: 18 March 2022
Published: 26 March 2022

Abstract: The Electro-Fenton (E-Fenton) technique has shown great potential in wastewater treatment, while the sustainable and continuing supply of $Fe2^+$ remains challenging. Herein, we demonstrate the construction of a novel E-Fenton system by magnetically decorating zero-valent iron (ZVI) onto a RuO_2-IrO_2/Ti (ZVI-RuO_2-IrO_2/Ti) electrode for high-efficient treatment of pharmaceutical wastewater, which is considerably refractory and harmful to conventional biological processes. By using ZVI as a durable source of Fe(II) irons, 78.69% of COD and 76.40% of TOC may be rapidly removed by the developed ZVI-RuO_2-IrO_2/Ti electrode, while the ZVI-RuO_2-IrO_2/Ti electrode using ZVI only reduces 35.64% of COD under optimized conditions at initial COD and TOC values of 5500 mg/L and 4300 mg/L, respectively. Moreover, the increase in BOD_5/COD from 0.21 to 0.52 highlights the enhanced biodegradability of the treated effluent. The analysis of a simultaneously formed precipitation on electrodes suggests that the coagulation process dominated by Fe^{3+}/Fe^{2+} also plays a non-negligible role in pharmaceutical wastewater treatment. In addition, the monitoring of the evolution of nitrogen elements and the formation of by-products in the E-Fenton process verifies its great capacity toward those organic pollutants found in pharmaceutical wastewater. Our study offers a practical solution for enhancing the performance of E-Fenton systems, and effectively treating refractory pharmaceutical wastewater.

Keywords: electro-oxidation; zero-valent iron; pharmaceutical wastewater; E-Fenton process

1. Introduction

Due to the rapidly increased consumption of pharmaceuticals in recent years, pharmaceutical effluent has been threatening both ecosystems and human health via accumulation in the environment and the food chain if it is not well treated [1–3]. Residue organic pollutant components in pharmaceutical effluent, such as harmful antibiotics and hormones, are usually difficult to destroy and/or mineralize [4]. On the other hand, pharmaceutical effluent shows high chemical oxygen demand (COD) and total organic carbon (TOC) values, and poor biodegradability, rendering conventional biological wastewater treatment useless [5]. Therefore, it is of great importance to develop an effective but low-cost method for treating pharmaceutical effluent [6,7].

Advanced oxidation processes (AOPs) are considered an efficient technology for enhancing the biodegradability of pharmaceutical wastewater prior to biological treatment by generating strong oxidizing agents, such as hydroxyl radicals (·OH) and sulfate radicals (SO_4^-) [8–10]. Hydroxyl radical-based AOPs such as Fenton/Fenton-like, E-Fenton, ozonation, and photocatalysis processes show promise in destroying toxic pharmaceuticals [3,11]. Among them, E-Fenton, coupling the chemical Fenton process with electrochemistry, has shown great potential for treating refractory wastewater due to its strong oxidation capacity, lower installation costs and easy operation [12]. In the E-Fenton process, the in-situ formed or added hydrogen peroxide (H_2O_2) may be converted into a large amount of unselective ·OH by the presence of Fe^{2+} [13,14]. As shown in Equations (1)–(3), the Fe^{2+} regenerating at the cathode through Equation (3) enables the rapid decomposition of H_2O_2 into highly reactive ·OH [15,16], where the regeneration efficiency of Fe^{2+} and decomposition of H_2O_2 play significant roles in the E-Fenton process [17].Besides, the high efficiency of the electrochemical process relies on the electrochemical properties of the anode materials [18]. As a powerful anodic oxidation material, boron-doped diamond (BDD) electrodes have been extensively used and investigated in the context on organic wastewater treatment [19–21]. However, due to the high cost of BDD, it is imperative to develop a potential alternative anode with low cost and easy fabrication.

$$O_2 + 2H^+ + 2e^- \rightarrow H_2O_2 \quad (1)$$

$$Fe^{2+} + H_2O_2 \rightarrow Fe^{3+} + \cdot OH + OH^- \quad (2)$$

$$Fe^{3+} + e^- \rightarrow Fe^{2+} \quad (3)$$

On the other hand, much effort has been made to improving the in-situ H_2O_2 formation performance of cathodes by designing various catalytic electrode materials [22,23]. For instance, the high efficiency treatment (98% Rhodamine B removal) of simulated organic wastewater was achieved in an E-Fenton system with a graphene/graphite-based gas diffusion electrode [24]. Aiming to enhance in-situ H_2O_2 production, a graphene modified carbon felt cathode was fabricated for the E-Fenton process, in which 75% of the antineoplastic drug used for cancer treatment could be totally mineralized [25]. Inspired by the function of photocatalysis, Orimolade et al., investigated the mineralization of paracetamol by coupling a cathodic E-Fenton process and an anodic photoelectrochemical system, obtaining 71% TOC removal efficiency [26]. However, the overall treatment efficiency of developed E-Fenton systems remains at a relatively slow kinetic state with short-term operation ability because the presence of Fe^{2+} is unsustainable.

As an environmental friendly material, zero-valent iron (ZVI) is considered an available source of Fe^{2+} for emerging environmental applications [27]. ZVI is able to release Fe^{2+} and avoid the rapid depletion of Fe^{2+} by reducing Fe^{3+} to Fe^{2+} via a rapid electron transfer [28]. The feasibility of using magnetically decorated ZVI as the source of Fe^{2+}, which is also an important factor in the E-Fenton process, has rarely been studied. Moreover, most E-Fenton processes are evaluated using synthetic organic wastewater and the treatment of real pharmaceutical wastewater has barely been reported [16]. Meanwhile, electrocoagulation, relying on the generated iron hydroxide aggregates for flocculation under an external electric field [29], is another important process when using the electrochemical oxidation method. Electrocoagulation exhibits high removal efficiency for suspended solids as well as total phosphorus (TP). For instance, a pure iron anode is a common electrocoagulation anode material [30]. As an anode in the E-Fenton process, ZVI may be converted to Fe^{2+}/Fe^{3+} for initiating effective coagulation to synergistically remove pollutants.

In this study, a TiO_2-RuO_2 coated titanium anode was employed as a model electrode for magnetically decorating ZVI in E-Fenton systems, aiming to improve the treatment efficiency of real pharmaceutical effluent. The ZVI-RuO_2-IrO_2/Ti composite electrode was firstly constructed for the E-Fenton process, whose capacity towards real pharmaceutical effluent treatment was systematically evaluated in terms of COD and TOC removal and

biodegradability. Specifically, the effects of operational parameters (i.e., initial pH, applied voltage, and ZVI dosage) on the efficiency of COD and TOC removal were examined. A control experiment was conducted by degrading tetracycline (TC) to test the ability of the E-Fenton process to degrade specific pharmaceutical compounds. The fluorescence method was employed to detect the ·OH concentration of the E-Fenton system. Fluorescence excitation-emission matrix (EEM) spectra were measured to analyze the degradation efficiency of organic substances in the effluent. Scanning electron microscopy-energy dispersive spectrometry (SEM-EDS), X-ray diffraction (XRD), and X-ray photoelectron spectroscopy (XPS) were employed to investigate the characteristics of the precipitation on the constructed electrode. The possible by-products of the organic pollutants were detected by gas chromatography-mass spectrometry (GC-MS).

2. Materials and Characterizations

2.1. Materials

All the chemicals used in this study were of analytical purity and purchased from Aladdin Chemical Co., Ltd. (Shanghai, China). Deionized water was used in all the experiments except the real pharmaceutical-wastewater-treatment tests. The micro-scale zero-valent iron powder (>99.9%) and graphite plates were purchased from Qinghe Chuanjia Welding Material Co., Ltd. (Xingtai, China) and Qingdao Baofeng Graphite Co., Ltd. (QingDao, China), respectively. The RuO_2-IrO_2/Ti plate was obtained from Qinghe Yunxuan Metal Materials Co., Ltd. (Xingtai, China). The mass ratio of Ru to Ir on the surface of the titanium plate approximately 8:2. The pharmaceutical wastewater was obtained from the sewage pool of YuMei Biological Technology Co., Ltd. (Hangzhou, China) and was stored at 4 °C in polyethylene containers. Before treatment, the wastewater was subjected to a thorough quality analysis and the results are summarized in Table 1.

Table 1. Main characteristics of the raw pharmaceutical wastewater used in this study.

Parameters	Values	Average
COD	5388–6292 mg/L	5840 mg/L
TOC	4154–4720 mg/L	4437 mg/L
BOD_5	1190–2300 mg/L	1945 mg/L
BOD_5/COD	0.21–0.35 mg/L	0.28 mg/L
Cl^-	0.10–0.18 mg/L	0.14 mg/L
TP	2.26–2.72 mg/L	2.49 mg/L
Phosphates	1.98–2.51 mg/L	2.25 mg/L
TN	396–422 mg/L	409 mg/L
NO_3^-	9.2–11.0 mg/L	10.1 mg/L
NO_2^-	<0.016 mg/L	<0.016 mg/L
NH_4^+	66.38–75.28 mg/L	70.83 mg/L
pH	4.69–4.86	4.77
Fe	<0.1 μg/L	<0.1 μg/L
Cu	<0.1 μg/L	<0.1 μg/L
Conductivity	2.25–2.28 mS/cm	2.26 mS/cm

2.2. Analysis and Characterization Methods

COD and TOC were analyzed using a Rapid COD analyzer (Lianhua Technology, Taizhou, China, 5B-3F) and a Liqui TOC II (Elementar) analyzer, respectively. The COD and TOC removal efficiency was calculated using Equation (4). The BOD_5 for all the samples was determined by the standard dilution and seeding method [31]. The pH of the samples was adjusted to 7.0 before adding the inoculum solution. The BOD_5 measurement was carried out at a temperature of 20 °C with the inorganic nutrient solution in a dark location for 5 days. The nutrient solution contained the following mineral (g/L) according to the method: $MgSO_4 \cdot 7H_2O$, 22.5; $CaCl_2$, 27.5; $FeCl_3$, 0.15; NH_4Cl, 2.0; Na_2HPO_4, 6.80; KH_2PO_4, 2.80. A 10 mg/L solution of N-allylthiourea was used as a nitrification inhibitor (2 mL per diluted sample) [32]. In the control experiment, the nutrient solution was replaced by

glutamic acid (150 mg/L) and glucose (150 mg/L) in the blank solution to eliminate the impact of the nitrification inhibitor and the nutrients. The sample was substituted by water in the blank solution and the other conditions were unchanged [33]. The concentration of ammonia–nitrogen was determined by the salicylic acid spectrophotometry method (HJ 536-2009) and (TU-1901). The concentrations of NO_2^- and NO_3^- were detected by ion chromatography (PuriMaster 5000). The total nitrogen (TN) was determined by the alkaline potassium persulfate digestion–UV spectrophotometric method. The Cl^- concentration was determined using the standard silver nitrate titration method.

The EEM spectra of the raw wastewater and treated sample were recorded on a fluorescence spectrophotometer (F-4600, Hitachi, Japan) using a 3-dimensional model. The XRD patterns of the resultant precipitate were recorded using a DX-2700 (Dandong Haoyuan Instrument) diffractometer with monochromatic Cu Ka irradiation in the 2θ angular regions between 10 °and 80 °. The surface morphology, atomic composition, and distribution of the precipitate were measured by a scanning electron microscope equipped with SEM/EDS (Inspect F50, FEI). XPS was carried using an X-ray photoelectron spectrometer (K-Alpha, Thermo Fisher Scientific, Shanghai, China). The identification of specific drugs in the pharmaceutical wastewater and byproducts during E-Fenton treatment was performed by a GC (Agilent 7890B)-MS (Agilent 5977A) with the Agilent 19091N-213. The analytical procedures included the following: the samples were extracted with ethyl acetate and then filtered by a 0.45 μm membrane. The pressure of the nitrogen carrier gas was set to 100 kPa. The temperatures of injector and detector were 220 °C and 280 °C, respectively. The column temperature was initially held at 60 °C for 2 min, and was subsequently increased to 180 °C at 15 °C min^{-1}, and then increased to 280 °C at 40 °C min^{-1}, with the final temperature being held for 10 min. The mass spectra of the peaks were compared with the GC-MS database with a standard library (NIST05).

$$\text{COD or TOC removal efficiency} = \frac{C_0 - C_t}{C_0} \times 100\% \quad (4)$$

where C_0 and C_t correspond to the initial COD/TOC concentration and the concentration after a period of time, respectively.

The concentration of ·OH produced in the E-Fenton reactor was obtained by measuring the generated fluorescent results from the selective reaction of coumarin with the ·OH electro-generated species. The fluorescence intensities were measured using a spectrofluorometer (GB 11893-89, China) with a 456 nm wavelength, and the concentration of ·OH was calculated based on the curve of the standard concentration [34]. The concentration of TC was determined after the sample was filtered with a 0.45 μm membrane under the condition of a spectrophotometer with a 355 nm wavelength. The concentration of TP was determined by ammonium molybdate spectrophotometry with a vertical pressure steam sterilizer (GB/T 11893-1989). The concentration of phosphates was determined according to standards of HJ84-2016. The NH_4^+-N concentration was determined by salicylic acid–hypochlorite spectrophotometry. The samples were filled through micron membrane filtration before the above detection. The pH solution was monitored and adjusted using a digital pH meter (METTLER TOLEDO).

2.3. Experimental Setup and Operation

In the current study, a mixed metal oxide (TiO_2-RuO_2) coated titanium anode was employed in an electrochemical system [35]. Ti/TiO_2-RuO_2 and Ti/TiO_2-RuO_2-IrO_2 anodes were used in electrochemical treatment and efficient TOC removal was achieved at an appreciable cost [36]. In the constructed E-Fenton system, the anode was constructed by magnetically adsorbing a certain amount of ZVI powder (0.8/1.0/1.2/1.4 g/L) onto 16 cm^2 (4 cm × 4 cm) area of a RuO_2-IrO_2/Ti plate. The ZVI powder was anchored on the surface of the RuO_2-IrO_2/Ti plate through a 5 × 10 × 0.5 cm sintered NdFeB magnet (surface magnetic field strength 2000 GS). A photographic image of the electrodes in the E-Fenton system is shown in Figure S1. The graphite plate was used as the cathode. The composite

anode was attached to the wall of the glass and the cathode was placed in a parallel position to the anode with an inter-electrode gap of 2 cm.

All the batch experiments were performed in a 0.8 L open undivided cell at room temperature (T = 298 ± 2 K) filled with 500 mL of pharmaceutical wastewater containing 0.05 M sodium sulfate. The pH was adjusted to a desired value (i.e., 2, 3, and 4) by adding 1 M H_2SO_4 solutions. The experiments were performed under an invariant voltage mode (constant current voltage). The electrodes were connected to a digital DC power supply (MAISHENG MS-3010D) providing current and voltage in the ranges of 0–10 A and 0–30 V, respectively. Homogenization of the solutions was assured by continuous stirring using an electric stirrer with Teflon coating rabble at 30 rpm in all the experiments. The experimental setup is shown in Figure 1. In each experiment, H_2O_2 (concentration of 11.15 mol/L) was added externally into the solution (at an average rate of 1.08 mL/L·h). After turning on the electric stirrer, the treatment was initiated under the constant voltage condition. At the desired time, water samples were collected for analysis.

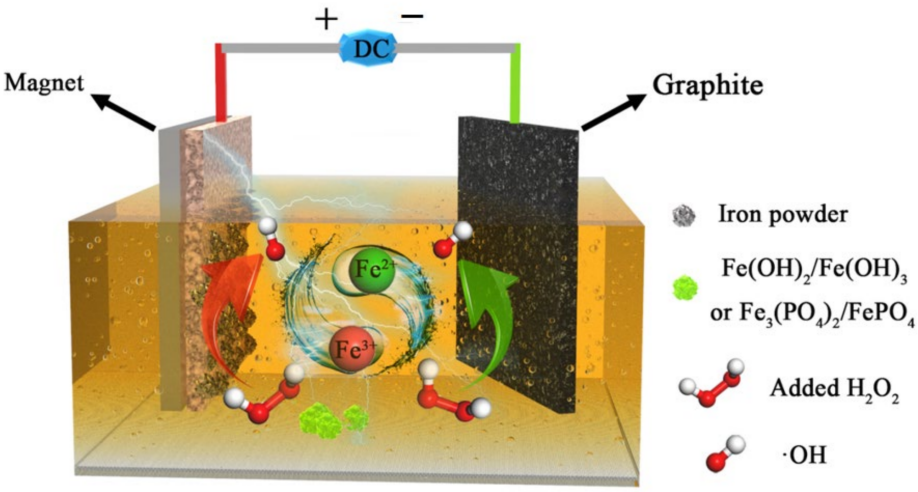

Figure 1. Schematic diagram of the experimental setup.

3. Results and Discussion

3.1. Influencing Factors of the Constructed Novel E-Fenton System

3.1.1. Initial pH Value

The impact of the initial pH value on the COD and TOC removal was evaluated by varying the initial pH value from 2 to 4 in the treatment experiments. It may be seen from Figure 2a,b that the initial pH value had a significant effect on the removal efficiency of COD and TOC in the E-Fenton process. The reduction of COD and TOC reached 65.71% and 57.39%, respectively after 12 h operation at an initial pH of 2.0. However, as the pH increased from 2.0 to 4.0, the COD and TOC removal decreased to 26.50% and 21.94%, respectively, which was much lower than that at a pH of 2.0.

The initial pH value may influence the E-Fenton reaction as the pH affects the concentration of Fe^{2+}, the formation of precipitate, and redox cycling between 2+ and 3+ states of iron. Relatively low pH values enhance the transformation from Fe^{3+} to Fe^{2+} and reduce $Fe(OH)_3$ precipitation. In addition, high Fe^{2+} concentrations improve the overall treatment efficiency because they act as an activator to promote the H_2O_2 decomposition into ·OH [37,38]. It may be observed that the generation rates of reddish-brown precipitates accelerated with the increase in the pH value during the E-Fenton process. The Fe^{3+} in the precipitate is hardly reconverted into Fe^{2+}, which compromises the Fe^{2+}/H_2O_2 ratio for continuing ·OH generation.

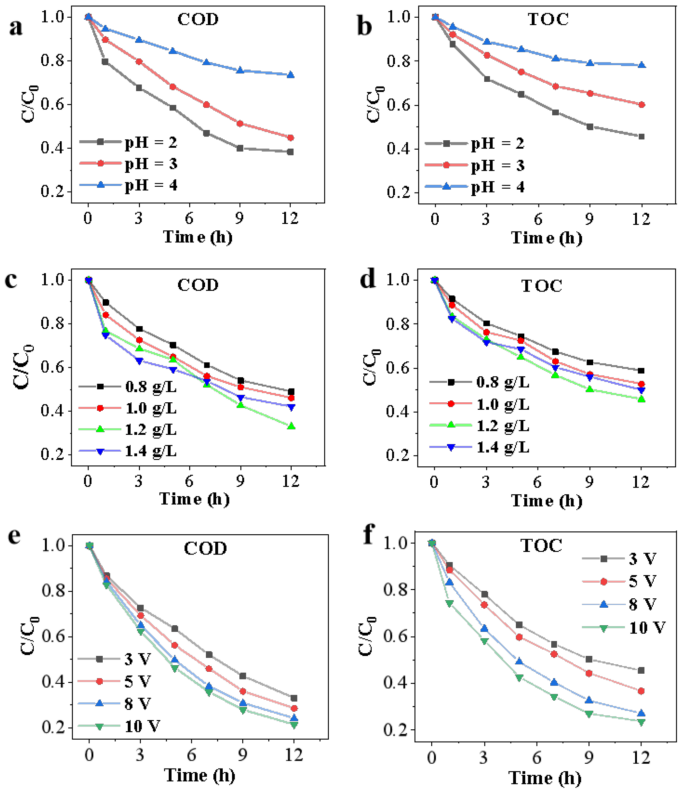

Figure 2. Effect of initial pH (**a**,**b**), (**c**,**d**) the dosage of ZVI, and the applied voltage (**e**,**f**) on COD and TOC removal percentage for the 500 mL solution.

In Figure S2, the pH value of the treated solution increases during the whole reaction, probably leading to a lower efficiency. The concentration of Fe^{3+} decreases since it turns into hydroxyl ($[Fe(OH)]^{2+}$, $[Fe(OH)_2]^{+}$, and $[Fe(OH)]^{4+}$) and hydroperoxy complexes ($[Fe(OH_2)_2]^{+}$ and $[Fe(OH)(HO_2)]^{+}$) at a relative high pH of 4.0. At a higher pH value, Fe^{3+} ions more readily form precipitates such as $Fe(OH)_3$, decreasing the free Fe^{2+} ions that may react with H_2O_2 and have a negative impact on the ·OH formation [39]. In addition, the pH value may influence the formation and decomposition rate of H_2O_2, which determines the production of radical ·OH [40]. Therefore, it is suggested to adjust the anaerobic digestion wastewater to a pH of 2.0 when applying the Fenton process for maximizing the treatment efficiency.

3.1.2. ZVI Dosage

The ratio of Fe^{2+}/H_2O_2 plays a crucial role in the removal rate of pollutants and the optimal ratio exhibits differing behavior in treating different types of wastewater [41]. To optimize the E-Fenton treatment process of the designed system, the COD and TOC removal efficiency of pharmaceutical wastewater was evaluated by varying the dosage of the initial ZVI (e.g., 0.8, 1.0, 1.2, and 1.4 g/L) under the same electro-chemical conditions (3 V at pH of 2). In batch experiments, H_2O_2 was added into the solution at an average rate of 1.08 mL/L·h. Before each experiment, the ZVI powder was combined with the anode plate and was consumed completely after the reaction (12 h). As may be seen in Figure 2c,d, an increase in the initial ZVI dosage from 0.8 g/L to 1.2 g/L may improve the degradation efficiency in terms of COD and TOC removal. The COD removal reached 51.04%, 53.97%, and 65.71%, respectively, while the TOC removal reached 42.26%, 49.33%, and 57.39%, respectively at 12 h. However, when the ZVI dosage rose to 1.4 g/L, the COD and TOC removal decreased to 57.93%, and 50.08%, respectively.

The ferrous ion proved to have a significant effect in the E-Fenton process as it catalyzes the decomposition of H_2O_2 into ·OH (Equation (3)). Therefore, an insufficient Fe^{2+}

concentration would prevent the formation of ·OH and H_2O_2 would accumulate, which undermines the degradation efficiency of refractory organics in the pharmaceutical wastewater. On the other hand, when the iron dosage was increased to 1.4 g/L, the concentration of ferrous ions in the system was so high that ·OH would be inevitably consumed by Fe^{2+} via Equation (5). Such a reaction competes over the organic pollutant degradation in the pharmaceutical wastewater by ·OH. In addition, the Fe^{2+} ions would turn into Fe^{3+} ions after reacting with ·OH, which is inactive for H_2O_2 decomposition. Therefore, the ·OH concentration would decrease if the Fe^{2+} concentration is too high and the removal efficiency of COD and TOC would be limited [37,41,42]. Therefore, a moderate Fe/H_2O_2 molar ratio favored the COD oxidation process in this study. The optimal dosage of ZVI was 1.2 g/L, while the ZVI/H_2O_2 molar ratio was 0.747:1 (a H_2O_2 concentration of 11.15 mol/L at rate of 0.27 mL/L·h).

$$Fe^{2+} + \cdot OH \rightarrow Fe^{3+} + OH^- \tag{5}$$

3.1.3. Applied Voltage

The ZVI was uniformly coated on the surface of the RuO_2-IrO_2/Ti plate with a needle shape area of 12 cm^2 after applying the magnetic field. It was difficult to accurately calculate the surface area and current density of the ZVI-RuO_2-IrO_2/Ti anode; therefore, this experiment was performed at a constant voltage mode. The influence of applied voltage, one of the key parameters in the E-Fenton process, on the treatment efficiency was investigated by changing it from 3 to10 V. It may be observed from Figure 2e,f that the higher the applied voltage, the better the TOC removal, without the existence of an optimal threshold value. The COD removal was 65.71%, 71.50%, 75.91%, and 78.69% while the TOC removal was 57.39%, 63.32%, 73.06%, and 76.40% at applied voltages of 3 V, 5 V, 8 V, and 10 V, respectively. Such differences in the treatment efficiency at various applied voltages were attributed to the accelerated electron transfer and promoted oxygen reduction reactions with the increase in applied potential, thereby promoting organic substance oxidation [43]. Moreover, the electrode reactions and removal rates were significantly improved due to the increased amounts of electrogenerated hydrogen peroxide, resulting in a higher production of ·OH [44,45]. When the applied voltage rose to 8 V, the COD removal showed a slight increase.

Energy consumption is one of the main components of the total cost, especially in electrochemical processes. The energy consumption (E) of the E-Fenton processes at voltages of 3 V, 5 V, 8 V, and 10 V were calculated from Equation (6) and the results are shown in Table S1. Although it is clear that the COD and TOC removal efficiency using a voltage of 10 V outperformed that of 3 V, the energy consumption would also be much higher, which would somehow undermine the treatment potential. Besides, a low energy consumption approach would be suitable for engineering treatment of wastewater in line with the recent "dual control of energy consumption" policy declared by the Chinese government. Regarding the net-cost and feasibility, we selected 3 V as the optimal voltage in the further studies, which considers both the cost and treatment efficiency.

$$E\left(\mathrm{kWh/m^3}\right) = \frac{\mathrm{VIt}}{\mathrm{v}} \tag{6}$$

where V (volt) is the potential difference, I (A) is the applied current, t is the reaction time (h), and v (m^3) is the volume of wastewater.

3.1.4. Na_2SO_4 Concentration

Figure 3a,b illustrates the removal efficiency of COD and TOC at different Na_2SO_4 concentrations in the wastewater (0, 0.025, and 0.050 mol/L). In batch experiments, the applied voltage was 3 V, the initial pH was 2.0, and the ZVI dosage was 1.2 g/L. The COD and TOC removal efficiency was 49.88% and 41.78%, respectively after 12 h treatment when Na_2SO_4 was 0 mol/L, which was lower than that of 0.025 mol/L (65.71% of COD and 57.39% of TOC). When the concentration of Na_2SO_4 was increased to 0.050 mol/L, the COD

and TOC removal efficiency increased slightly. The concentration of Na_2SO_4 affects the conductivity of the solution, which limits the oxidation efficiency of the E-Fenton process. A value of 0.025 mol/L was selected as the optimal Na_2SO_4 concentration as a higher dosage of Na_2SO_4 results in almost unchanged removal.

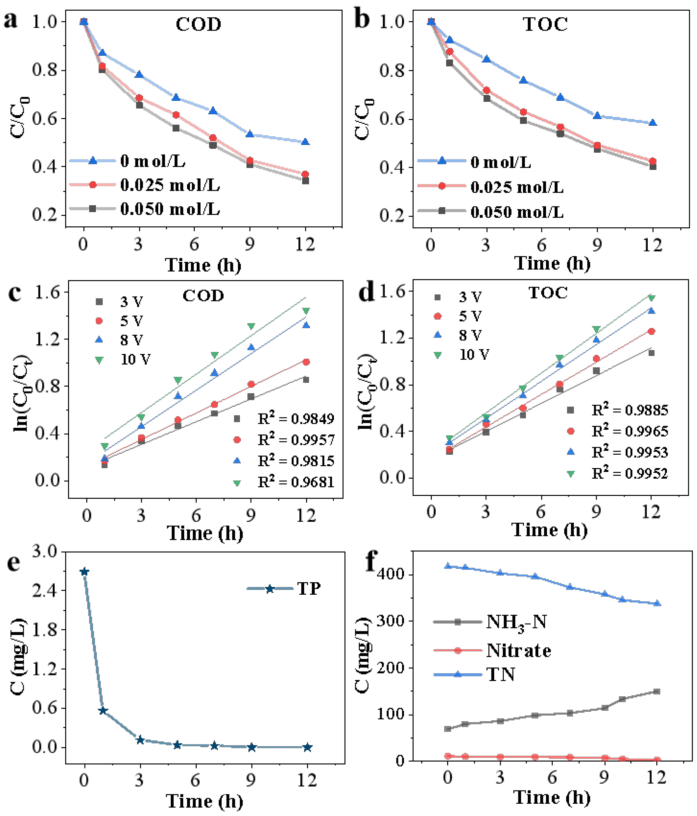

Figure 3. (**a**,**b**) Effect of the Na_2SO_4 concentration on the COD and TOC removal percentage. (**c**,**d**) The kinetics of COD and TOC removal at different voltages. (**e**,**f**). The TP concentration changes with time and the NH_3-N, nitrate and TN concentrations change with time.

3.2. Kinetics of COD and TOC Removal

To understand the kinetics of COD and TOC removal in the E-Fenton process, the experimental data at different voltages were fitted with pseudo zero, pseudo-first, or pseudo-second order kinetics. In the removal of COD and TOC, the pseudo-first order kinetic model fitted the experimental data better than both the pseudo-zero order and pseudo second order kinetic models. As shown in Figure 3c,d, the pseudo-first order rate constant increased with increased voltage. The rate constants are shown in Table S2 in the supporting information. The removal efficiency was expressed as the equation:

$$\frac{dC}{dt} = -\mathrm{kC} \tag{7}$$

After integration, the above equation gave:

$$\ln\left(\frac{C_0}{C_t}\right) = kt \tag{8}$$

where C_0 and C_t correspond to the initial COD/TOC concentration and the concentration after a period of time, respectively.

3.3. Overall Treatment Efficiency under Optimal Conditions

3.3.1. Total Phosphorous Removal

As shown in Table 1, the content of TP was 2.03–2.69 mg/L, which was higher than the prescribed discharge standard (China) with the value of 0.5 mg/L (GB 18918-2002). The phosphate concentration was detected to be 2.51 mg/L, while the TP was 2.69 mg/L, indicating that most of the P element exists in the form of phosphates in the pharmaceutical wastewater. The concentrations of TP during the E-Fenton treatment are shown in Figure 3e. In the experiment, the applied voltage was 3 V, the initial pH was 2.0, the ZVI dosage was 1.2 g/L, and the Na_2SO_4 concentration was 0.025 mol/L. The TP removal efficiency was above 90% after 3 h and was nearly 100% after 12 h of treatment. The removal performance of TP was high in the E-Fenton process as the phosphate was trapped by Fe^{3+} via the formation of an iron phosphate precipitate (Equation (9)). Moreover, the low concentration of organophosphorus in the pharmaceutical wastewater may be oxidized to phosphate under the combined action of ions and radical ·OH [44].

$$Fe^{3+} + H_nPO_4{}^{(3-n)^-} \rightarrow FePO_4 \downarrow + nH^+ \quad (9)$$

3.3.2. Transformation of Nitrogen and Its Species

The transformation of nitrogen during the degradation process was investigated to analyze the nitrogen conversion of the E-Fenton system. The degradation of organics was accompanied by the formation of ammonium ions and nitrate. Figure 3f presents in nitrogen (mainly in the form of nitrates, $NO_3{}^-$, and ammonium ions, $NH_4{}^+$) concentrations under optimal conditions (the applied voltage was 3 V, the initial pH was 2.0, the ZVI dosage was 1.2 g/L, and the Na_2SO_4 concentration was 0.025 mol/L). The concentration of ammonia–nitrogen (NH_3-N) increased from 69.1 to 147.7 mg/L in 12 h, corresponding to the production of ammonium ions during oxidative ring opening of aromatic intermediates [46]. Moreover, the decrease in $NO_3{}^-$ from 11.7 to 2.95 mg/L indicated that the nitrates may be transformed into gaseous nitrogen species during the E-Fenton process [47]. The TN declined from 419 to 329 mg N/L at the end of electrolysis, indicating that a small part of the organic nitrogen was volatilized in the form of NO_x, N_2, and chloramines during the mixing [46,48]. Because of the high concentration of ammonia nitrogen, it is necessary to combine the E-Fenton process with a biological method to remove the NH_3-N. In the application of industrial pharmaceutical wastewater treatment, physical and chemical methods are always employed to pretreat wastewater and biological methods are combined for deep treatment.

3.3.3. Removal Performance of Tetracycline

As a broad-spectrum antimicrobial-activity antibiotic, tetracycline (TC) plays a vital role in human healthcare and husbandry [49]. A control experiment was conducted by degrading TC (conditions: initial pH = 2.0, applied voltage = 3 V, iron powder = 1.2 g/L, Na_2SO_4 concentration = 0.025 mol/L) to test the ability of the E-Fenton process ton degrade specific pharmaceutical compounds. The removal efficiency of TC is shown in Figure S3. For the TC solution with an initial concentration of 100 mg/L, the removal rate reached 85.6% and 98.8% after 1 and 2 h reaction, respectively, which showed great performance in terms of TC removal. The results compared with those of the TC degradation efficiency obtained by other reports using E-Fenton are shown in Table S3 [50–52]. Although a high mineralization rate of TC was achieved on the BDD anode, it makes great sense to employee replacement cost-effective electrodes considering the equipment costs [53].

3.4. Biodegradability Analysis

The BOD_5/COD ratio that represents the biodegradability of wastewater was measured to determine the feasibility of biological pretreatment for the treated pharmaceutical wastewater subjected to the E-Fenton ment. AOPs have been generally proposed as auxiliary methods to condition refractory wastewater as pre- or post-treatment in order to

degrade bio-recalcitrant pollutants [54,55]. As shown in Figure 4a, the raw wastewater had a BOD_5/COD ratio of 0.21, which was lower than the general biodegradability threshold (0.4) for biological treatment [56]. After 6 h of treatment in the E-Fenton process, the wastewater became easily biodegradable with a BOD_5/COD ratio of 0.45, which was higher than the threshold. After 6 h treatment in the E-Fenton process, the wastewater became easily biodegradable with a BOD_5/COD ratio of 0.45, which was higher than the threshold. After 12 h treatment, the biodegradability of the effluent increased to 0.52. Therefore, the designed E-Fenton system has the potential for use as the pretreatment of pharmaceutical wastewater to ensure the feasibility of subsequent biological units. Since engineering factors such as the pH value, nutrients, temperature, and nitrification are vital for the BOD_5 results, future studies are needed to uncover the specific influences of these factors on the BOD_5 values.

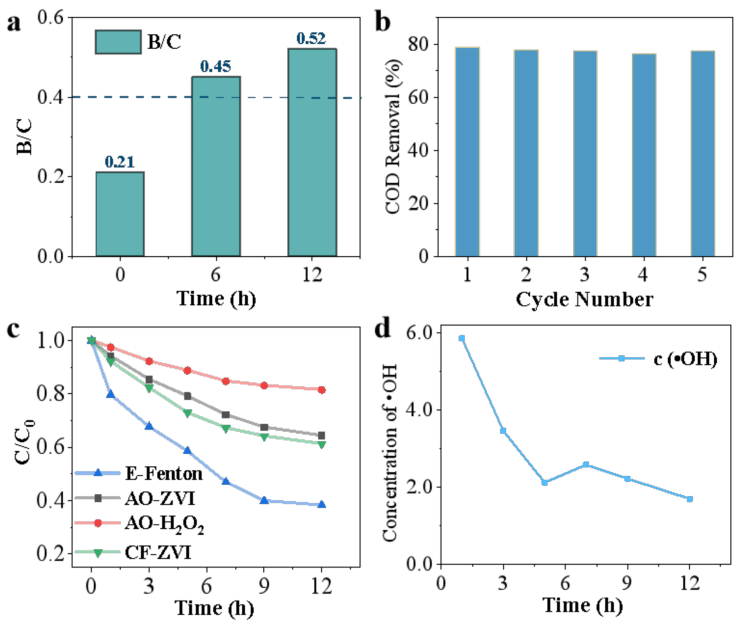

Figure 4. (**a**) Changes in the BOD_5/COD ratio over treatment time; (**b**) Reusability of the anode material; (**c**) COD removal percentage changes in four treatment models: AO-H_2O_2, AO-ZVI, CF-ZVI, and E-Fenton processes. (**d**) Changes in the·OH concentration. Conditions: initial pH = 2.0, applied voltage = 3 V, iron powder = 1.2 g/L, Na_2SO_4 concentration = 0.025 mol/L.

3.5. Reusability of Anode Material

One of the advantages of using the RuO_2-IrO_2/Ti electrode is its reusability. Based on the degradation conditions with an initial pH of 2.0, an applied voltage of 10 V, an iron dosage of 1.2 g/L, and a Na_2SO_4 concentration of 0.025 mol/L, the durability of the anode was evaluated in the pharmaceutical wastewater treatment. As shown in Figure 4b, the final removal rate of COD showed almost no reduction in five cycles of degradation, indicating the good stability and reusability of the anode material in the E-Fenton system.

3.6. Treatment Mechanism Clarifications

3.6.1. Role of Additional H_2O_2

Control experiments were performed in different systems to explore the role of the additional H_2O_2 and ZVI in the system. In the anodic oxidation–H_2O_2 (AO-H_2O_2) process, no ZVI was anchored on the anode plate. Carbon felt (CF) has a larger surface area than graphite and is commonly used in typical E-Fenton systems [57]. In the CF-ZVI process, CF was used instead of graphite as the cathode with no additional H_2O_2. Moreover, no H_2O_2 was added in the anodic oxidation-ZVI (AO-ZVI) process. The other conditions of the AO-H_2O_2 and AO-ZVI processes were consistent with the E-Fenton process. The

AO-H_2O_2 process was used to clarify the sole role of H_2O_2 in pollutant degradation in the system without ZVI. In this case, the COD was removed mainly by the oxidation function of H_2O_2 itself. The COD removal efficiency of batch experiments is shown in Table S4 and Figure 4c. In the E-Fenton process, the COD removal reached 65.71% of treatment while only 18.48% of COD was removed in the absence of ZVI. The COD removal efficiency was 35.64% and 38.70% in the CF-ZVI and AO-ZVI process, respectively, confirming that coagulation impacted the apparent COD removal rate [58]. This indicated that high contaminant removal is not achievable when the H_2O_2 acts alone without iron power. The COD removal efficiency of CF-ZVI was higher than AO-ZVI because the CF cathode helped to generate ·OH during electrolysis to degrade part of the organics [59]. Moreover, the selected pharmaceutical wastewater is hard to treat so the COD removal efficiency of CF-ZVI was not able to reach the ideal level. This observation suggests that the ·OH formed by external H_2O_2 decomposition in the E-Fenton process played a crucial role in the organic degradation/mineralization.

3.6.2. The Concentration of ·OH

The ·OH concentrations detected by the fluorescence method of the E-Fenton system are shown in Figure 4d. In the first hour of the reaction, the ·OH concentration reached maximum values of 5.25 μmol/L, which represents a high level compared with those obtained by other authors using E-Fenton and coumarin as a probe molecule [60–62]. The ·OH concentration rapidly decreased to 2.12 μmol/L due to the decomposition of the added H_2O_2. The ·OH concentration increased to 2.70 μmol/L, which could have been related to the conversion between Fe^{3+} and Fe^{2+}. This result further proves the dominant role of ·OH formed by the addition H_2O_2 and that the generation of ·OH is controlled by the presence of H_2O_2 and Fe^{2+} [63].

3.6.3. Three-Dimensional Fluorescence Analysis

Figure 5a depicts the detailed three-dimensional fluorescence spectra of the pharmaceutical wastewater before and after treatment with the E-Fenton systems (conditions: initial pH = 2.0, applied voltage = 3 V, iron powder = 1.2 g/L, Na_2SO_4 concentration = 0.025 mol/L). Three main fluorescence peaks were observed in the spectrum of the untreated sample: Peak A (E_x/E_m around 240/350 nm) was detected region I, and corresponded to aromatic-like proteins [64]; Peak B (E_x/E_m at around 275/355 nm) was detected in region III, and was assigned to protein that was rich in tryptophan [65]; and peak C (E_x/Em around 290/350 nm) shown in region III was ascribed to humic acid-like substances [66]. After treatment in the E-Fenton system for 12 h, the fluorescence intensities of these three peaks were clearly reduced, as shown in Figure 5b. The humic-like substances, aromatic-like proteins, and tryptophan may be effectively degraded by the constructed experiment. This demonstrates that most of the organic substance may be removed with the E-Fenton process.

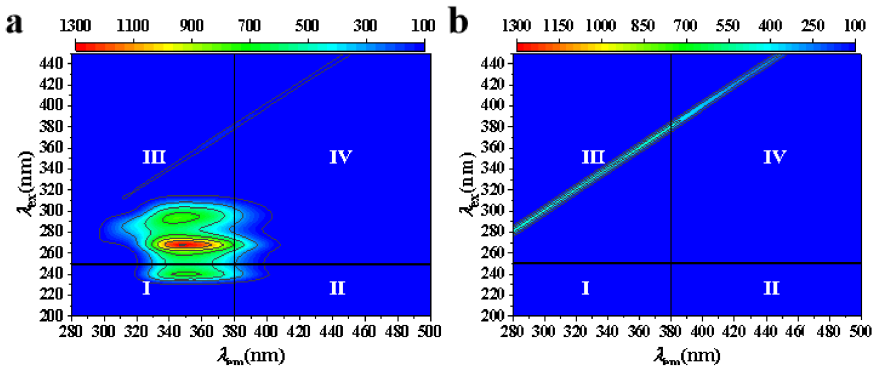

Figure 5. Three-dimensional-EEM spectra of (**a**) the pharmaceutical wastewater and (**b**) the treated sample.

3.6.4. Precipitate Characterization

To further explore the electrocoagulation mechanism of TP and organic substance degradation, the morphology and elemental composition of the precipitate were investigated by scanning electron microscopy equipped with energy dispersive spectrometry (SEM-EDS) and a SEM magnification of 10,000. As shown in Figure 6a, the collected precipitation had an irregular shape with a rough and uncompact surface. It is observed from the EDS elemental mapping images (Figure 6b) that the precipitation contained S (2.59%), C (4.28%), N (0.76%), O (38.77%), Fe (51.94%), and P (1.66%). It may be confirmed that metal hydroxides served mainly as a coagulant both for adsorbing some of the organics and for removing phosphorus via the synergistic coagulation process with E-Fenton.

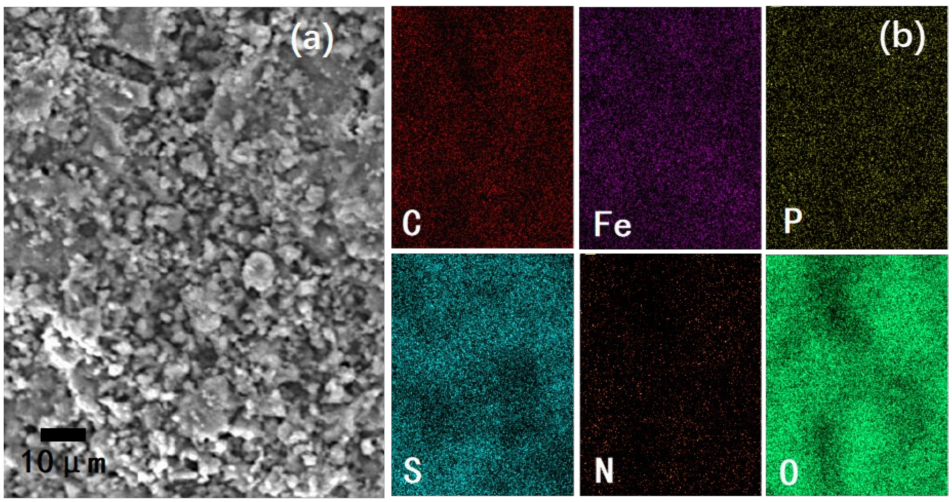

Figure 6. SEM image (**a**) and elemental maps (**b**) of the precipitate after treatment. Conditions: initial pH = 2, applied voltage = 3 V, iron powder = 1.2 g, Na_2SO_4 concentration = 0.025 mol/L.

The crystalline structure and composition of the precipitation were identified by X-ray diffraction (XRD) patterns (Figure S4). It may be observed that the sample has an amorphous nature with no distinct characteristic peaks, which may indicate the presence of iron oxides. The detection of iron oxides is not easy due to their amorphous structure [67]. Further analysis of the precipitation was then performed by XPS. Figure 7a shows the XPS survey spectrum and Figure 7b–f shows the high-resolution XPS spectra of each element present in the precipitate (C 1s, Fe 2p, N 1s, S 2p, P 2p, and O 1s). In Figure 7b, three peaks at 284.8, 286.7 and 288.7 eV are assigned to C-C, C=O, and C-O=C, respectively. The presence of C highlights the adsorption of some organic compounds by precipitates during the coagulation process [68]. The O1 s spectra (Figure 7c) may be deconvoluted into three peaks at 530.1, 531.8 and 534.3 eV, respectively. The peaks at 531.8 eV and 534.3 eV are attributed to Si-O and adsorbed molecular water (H-O-H), respectively [69,70]. The peak at 530.1 eV represented the metal–oxygen bonds, in agreement with the presence of iron hydroxides [71]. Figure 7d shows four clear satellite peaks and that the distance between Fe $2p_{3/2}$ and Fe $2p_{1/2}$ was 13.6 eV. The appearance of peaks of 712.0 eV and 725.4 eV represents Fe(II) while the others at 714.8 eV and 725.4 eV belonged to Fe(III), indicating the coexistence of Fe(II)/Fe(III) on the precipitate after the E-Fenton process [70]. As shown in Figure 7f, the peaks at 132.8 eV and 133.8 eV correspond to +3 and +5 of phosphorus, respectively, which indicates the presence of HPO_3^{2-} and HPO_4^{2-} on the surface of the precipitation [72]. The S element on the precipitation (Figure 7e) may be ascribed to the added electrolyte (Na_2SO_4).

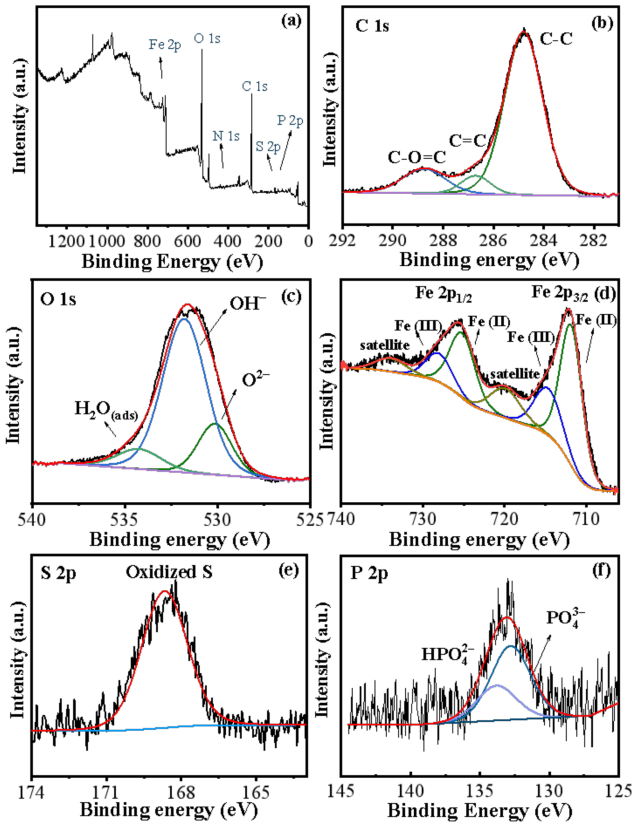

Figure 7. XPS spectra of the surface elements of the precipitate after treatment: (**a**) survey spectrum, (**b**) C element, (**c**) O element, (**d**) Fe element, (**e**) S element, and (**f**) P element. Conditions: initial pH = 2, applied voltage = 3 V, iron powder = 1.2 g/L, Na_2SO_4 concentration = 0.025 mol/L. The black lines refer to the raw data of XPS while the colored lines refer to the deconvoluted peaks.

According to Figure 4c, in the AO-ZVI process (no additional H_2O_2), the COD removal efficiency was 35.64%. It can be speculated that electrocoagulation can remove a part of the organic substances in the system. The XPS spectra (Figure 7) show the presence of HPO_3^{2-}/HPO_4^{2-} and Fe(II)/Fe(III) on the surface of the precipitate after the reaction, which indicates that the iron flocculant produced by dissolved anodic is able to remove the pollutants. This proves that the electrocoagulation process had high efficiency in terms of phosphate removal in this system. In the constructed E-Fenton system, refractory organic pollutants were mainly degraded by the combination of ·OH and electrocoagulation [44].

3.6.5. Byproducts and Possible Degradation Pathway

To gain insight into the possible degradation mechanism, intermediates generated in the E-Fenton process were monitored by GC-MS. Five organic compounds verified in the raw wastewater are presented in Table 2. The chromatogram patterns of the five organic compounds are shown in Figure S5. The pyrazoles are important intermediates for the synthesis of various heterocyclic compounds and have a wide range of applications in pharmaceutical synthesis [73]. The polydimethylsiloxanes may serve as the active pharmaceutical ingredient, the excipient, or the matrix in the drug delivery system. The pharmaceutical formulations formed with silicon dioxide may eliminate foam and eliminate flatulence as well as other stomach ailments [74]. Synthetic phenolic antioxidants (SPAs) have been extensively applied in a variety of products including cosmetics, plastics, pharmaceuticals, and foodstuffs. As one type of SPA, 2,2′-methylenebis (6-tert-butyl-4-methylphenol)(AO2246) was reported to have apparent reproductive toxicity [75–77]. Moreover, AO2246 has larger aquatic toxicities than hydroxyanisole, butylated hydroxytoluene, and tert-butyl hydroquinone [75].

Table 2. Five organic compounds verified in the raw wastewater detected by GC-MS.

Molecular Structures	Substance Names	Retention Time (Min)
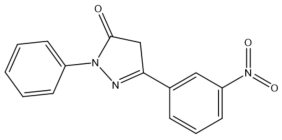	5-(3-nitrophenyl)-2-phenyl-2,4-dihydro-3H-pyrazol-3-one	6.021
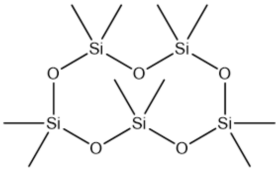	Decamethylcyclopentasiloxane	7.950
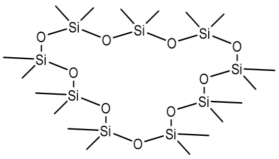	6,6′-methylenebis(2-(tert-butyl)-4-methylphenol)	13.545
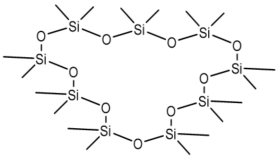	2,2,4,4,6,6,8,8,10,10,12,12,14,14,16,16,18,18-octadecamethyl-1,3,5,7,9,11,13,15,17-nonaoxa-2,4,6,8,10,12,14,16,18-nonasilacyclooctadecane	14.095
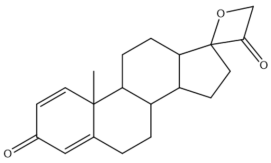	10,13-dimethyl-7,8,9,10,11,12,13,14,15,16-decahydrospiro[cyclopenta[a]phenanthrene-17,2′-oxetane]-3,3′(6H)-dione	15.995

Although not all compounds were identified in the 12 h treatment since the organic species were changeable, many organic compounds are detectable by GC-MS [78]. Information on the by-products detected by GC-MS after the E-Fenton process (conditions: initial pH = 2.0, applied voltage = 3 V, iron powder = 1.2 g/L, Na_2SO_4 concentration = 0.025 mol/L) is shown in Table S5. According to the molecular structures of the detected intermediates, the possible degradation pathway is proposed in Figure 8. The high-molecule cyclic polydimethylsiloxanes and aromatic substances were degraded after the reaction. It may be speculated that the formation of long-chain organic intermediates was a result of ring-opening and chain-breaking effects on macromolecular organic compounds. High-level organic compounds were oxidized into low-molecular weight organic compounds such as 2-(dimethylamino)acetaldehyde, 2-hydroxyethyl acetate, pyrrolidine-2,5-dione, and o-xylene during the E-Fenton process. A part of these intermediates was further transformed into NO_x and N_2, escaping from the E-Fenton system according to the above analysis.

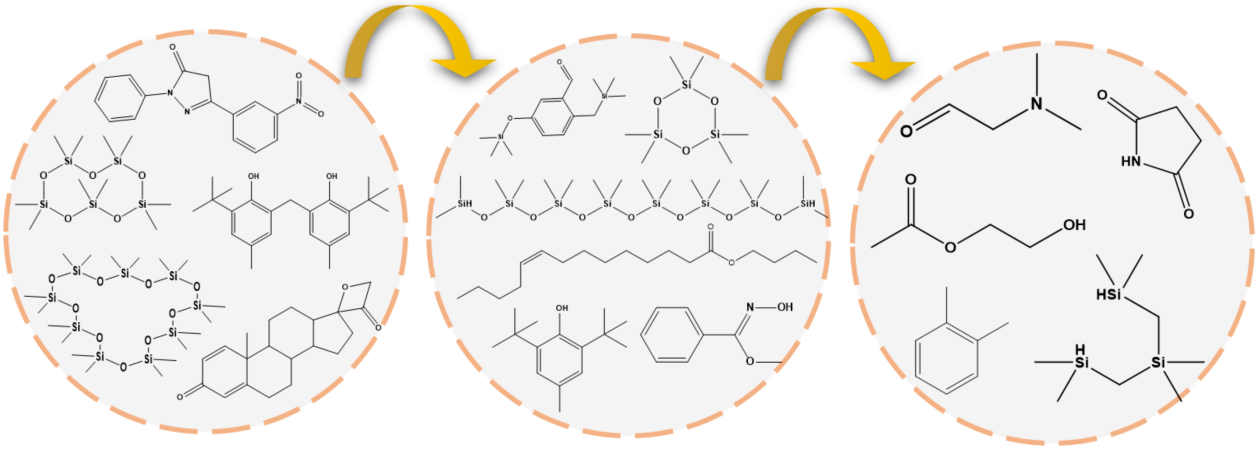

Figure 8. Proposed mineralization pathway followed by the main organic pollutants found in the actual pharmaceutical wastewater.

4. Conclusions

In summary, we demonstrated the successful construction of a novel E-Fenton system by magnetically decorating ZVI onto a RuO_2-IrO_2/Ti electrode, enabling the high-efficient treatment of pharmaceutical wastewater due to the unique role of ZVI in the continuing supply of Fe(II) ions. Refractory organic pollutants in the wastewater were rapidly destroyed and mineralized in the novel E-Fenton system by the generated ·OH, while the conventional system showed a weaker ability to improve the biodegradability. The experimental results showed that decreasing the initial pH value, raising the applied voltage, and increasing the ZVI dosage had significant positive effects on COD and TOC removal. In addition, our constructed E-Fenton system also allowed for quick (12 h) and thorough TP removal (almost 100%) by the precipitation of phosphate with iron ions under the optimal conditions. Conversely, this system exhibited a moderate total nitrogen transformation capacity despite 74.8% of the nitrates being reduced into other nitrogen species and a part of nitrogen being removed in the form of N_2. This work highlights the great practicability potential of the novel constructed E-Fenton system for refractory and toxic pharmaceutical wastewater treatment. In the future, cathode materials efficiently producing H_2O_2 will be explored to reduce the dosage of H_2O_2. The development of E-Fenton reactors with a larger capacity will also be given more attention for the application of industrial wastewater treatment.

Supplementary Materials: The following supporting information can be downloaded at: https://www.mdpi.com/article/10.3390/w14071044/s1, Figure S1: The photographic image of the electrodes in the E-Fenton system; Figure S2: pH changes of the solution at initial pH of 2.0, 3.0 and 4.0. Conditions: applied voltage = 3 V, iron powder = 1.2 g/L; Figure S3: The removal efficiency of TC changes with time. Conditions: initial pH = 2.0, applied voltage = 3 V, iron powder = 1.2 g/L; Figure S4: XRD patterns of the precipitation sample after the treatment; Figure S5: The chromatograms and five organic compounds patterns of the raw pharmaceutical wastewater; Table S1: Energy consumption and removal efficiency of COD and TOC at different voltages; Table S2: The pseudo-first order rate constants of different voltages; Table S3: The removal efficiency of TC compared with other studies; Table S4: The COD removal efficiency of batch experiments; Table S5: The GC-MS results of the by-products during the wastewater treatment.

Author Contributions: M.D.: Writing—original draft, Data curation, Formal analysis, Validation, Investigation, Software, Methodology. D.Y.: Writing—original draft, Conceptualization, Methodology, Project administration, Funding acquisition, Writing—review and editing, Supervision, Resources, Methodology. S.G.: Investigation. G.L.: Investigation, Software. D.S.: Investigation. K.W.: Formal analysis. M.P.: Investigation, Software. T.Y.: Investigation, Writing—review and editing. All authors have read and agreed to the published version of the manuscript.

Funding: This work was funded by the National Natural Science Foundation of China (No. 22106141), the Start-up Funding of Zhejiang Sci-Tech University and the Postdoctoral Program (No. TYY202103) of Zhejiang Sci-Tech University Tongxiang Research Institute.

Institutional Review Board Statement: Not applicable.

Informed Consent Statement: Not applicable.

Data Availability Statement: The data presented in this study are available on request from the corresponding author.

Acknowledgments: Publishing of the results was financially supported by the Ministry of Education, Youth and Sports of the Czech Republic and the European Union (European Structural and Investment Funds—Operational Programme Research, Development and Education) in the frames of the project "International Research Laboratories", Reg. No. CZ.02.2.69/0.0/0.0/18_054/0014685.

Conflicts of Interest: The authors declare no conflict of interest.

References

1. Jiang, Y.; Shi, X.; Ng, H.Y. Aerobic granular sludge systems for treating hypersaline pharmaceutical wastewater: Start-up, long-term performances and metabolic function. *J. Hazard. Mater.* **2021**, *412*, 125229. [CrossRef] [PubMed]
2. Ji, J.; Gao, T.; Salama, E.-S.; El-Dalatony, M.M.; Peng, L.; Gong, Y.; Liu, P.; Li, X. Using Aspergillus niger whole-cell biocatalyst mycelial aerobic granular sludge to treat pharmaceutical wastewater containing β-lactam antibiotics. *Chem. Eng. J.* **2021**, *412*, 128665. [CrossRef]
3. Ao, X.-W.; Eloranta, J.; Huang, C.-H.; Santoro, D.; Sun, W.-J.; Lu, Z.-D.; Li, C. Peracetic acid-based advanced oxidation processes for decontamination and disinfection of water: A review. *Water Res.* **2021**, *188*, 116479. [CrossRef] [PubMed]
4. Huang, Y.; Jiang, J.; Ma, L.; Wang, Y.; Liang, M.; Zhang, Z.; Li, L. Iron foam combined ozonation for enhanced treatment of pharmaceutical wastewater. *Environ. Res.* **2020**, *183*, 109205. [CrossRef]
5. Li, C.; Mei, Y.; Qi, G.; Xu, W.; Zhou, Y.; Shen, Y. Degradation characteristics of four major pollutants in chemical pharmaceutical wastewater by Fenton process. *J. Environ. Chem. Eng.* **2021**, *9*, 104564. [CrossRef]
6. Ling, L.; Liu, Y.; Pan, D.; Lyu, W.; Xu, X.; Xiang, X.; Lyu, M.; Zhu, L. Catalytic detoxification of pharmaceutical wastewater by Fenton-like reaction with activated alumina supported CoMnAl composite metal oxides catalyst. *Chem. Eng. J.* **2020**, *381*, 122607. [CrossRef]
7. Kantar, C.; Oral, O.; Oz, N.A. Ligand enhanced pharmaceutical wastewater treatment with Fenton process using pyrite as the catalyst: Column experiments. *Chemosphere* **2019**, *237*, 124440. [CrossRef]
8. Chávez, A.M.; Gimeno, O.; Rey, A.; Pliego, G.; Oropesa, A.L.; Álvarez, P.M.; Beltrán, F. Treatment of highly polluted industrial wastewater by means of sequential aerobic biological oxidation-ozone based AOPs. *Chem. Eng. J.* **2019**, *361*, 89–98. [CrossRef]
9. Xie, Z.-H.; Zhou, H.-Y.; He, C.-S.; Pan, Z.-C.; Yao, G.; Lai, B. Synthesis, application and catalytic performance of layered double hydroxide based catalysts in advanced oxidation processes for wastewater decontamination: A review. *Chem. Eng. J.* **2021**, *414*, 128713. [CrossRef]
10. Kilic, M.Y.; Abdelraheem, W.H.; He, X.; Kestioglu, K.; Dionysiou, D.D. Photochemical treatment of tyrosol, a model phenolic compound present in olive mill wastewater, by hydroxyl and sulfate radical-based advanced oxidation processes (AOPs). *J. Hazard. Mater.* **2019**, *367*, 734–742. [CrossRef]
11. Bansal, P.; Verma, A.; Talwar, S. Detoxification of real pharmaceutical wastewater by integrating photocatalysis and photo-Fenton in fixed-mode. *Chem. Eng. J.* **2018**, *349*, 838–848. [CrossRef]
12. Li, D.; Zheng, T.; Liu, Y.; Hou, D.; He, H.; Song, H.; Zhang, J.; Tian, S.; Zhang, W.; Wang, L.; et al. A cost-effective Electro-Fenton process with graphite felt electrode aeration for degradation of dimethyl phthalate: Enhanced generation of H_2O_2 and iron recycling that simultaneously regenerates the electrode. *Chem. Eng. J.* **2020**, *394*, 125033. [CrossRef]
13. Monteil, H.; Péchaud, Y.; Oturan, N.; Oturan, M.A. A review on efficiency and cost effectiveness of electro- and bio-electro-Fenton processes: Application to the treatment of pharmaceutical pollutants in water. *Chem. Eng. J.* **2019**, *376*, 119577. [CrossRef]
14. Ye, Z.; Schukraft, G.E.M.; L'Hermitte, A.; Xiong, Y.; Brillas, E.; Petit, C.; Sirés, I. Mechanism and stability of an Fe-based 2D MOF during the photoelectro-Fenton treatment of organic micropollutants under UVA and visible light irradiation. *Water Res.* **2020**, *184*, 115986. [CrossRef]
15. Divyapriya, G.; Srinivasan, R.; Nambi, I.M.; Senthilnathan, J. Highly active and stable ferrocene functionalized graphene encapsulated carbon felt array—A novel rotating disc electrode for electro-Fenton oxidation of pharmaceutical compounds. *Electrochim. Acta* **2018**, *283*, 858–870. [CrossRef]
16. Mousset, E.; Pontvianne, S.; Pons, M.-N. Fate of inorganic nitrogen species under homogeneous Fenton combined with electro-oxidation/reduction treatments in synthetic solutions and reclaimed municipal wastewater. *Chemosphere* **2018**, *201*, 6–12. [CrossRef]
17. Qi, H.; Sun, X.; Sun, Z. Porous graphite felt electrode with catalytic defects for enhanced degradation of pollutants by electro-Fenton process. *Chem. Eng. J.* **2021**, *403*, 126270. [CrossRef]

18. Ouarda, Y.; Trellu, C.; Lesage, G.; Rivallin, M.; Drogui, P.; Cretin, M. Electro-oxidation of secondary effluents from various wastewater plants for the removal of acetaminophen and dissolved organic matter. *Sci. Total Environ.* **2020**, *738*, 140352. [CrossRef]
19. He, Y.; Lin, H.; Guo, Z.; Zhang, W.; Li, H.; Huang, W. Recent developments and advances in boron-doped diamond electrodes for electrochemical oxidation of organic pollutants. *Sep. Purif. Technol.* **2019**, *212*, 802–821. [CrossRef]
20. García-Gómez, C.; Drogui, P.; Zaviska, F.; Seyhi, B.; Gortáres-Moroyoqui, P.; Buelna, G.; Neira-Sáenz, C.; Estrada-Alvarado, M.; Ulloa-Mercado, R. Experimental design methodology applied to electrochemical oxidation of carbamazepine using Ti/PbO_2 and Ti/BDD electrodes. *J. Electroanal. Chem.* **2014**, *732*, 1–10. [CrossRef]
21. Kurt, U.; Apaydin, O.; Gönüllü, M.T. Reduction of COD in wastewater from an organized tannery industrial region by Electro-Fenton process. *J. Hazard. Mater.* **2007**, *143*, 33–40. [CrossRef] [PubMed]
22. Chai, Y.; Qin, P.; Wu, Z.; Bai, M.; Li, W.; Pan, J.; Cao, R.; Chen, A.; Jin, D.; Peng, C. A coupled system of flow-through electro-Fenton and electrosorption processes for the efficient treatment of high-salinity organic wastewater. *Sep. Purif. Technol.* **2021**, *267*, 118683. [CrossRef]
23. Ismail, S.A.; Ang, W.L.; Mohammad, A.W. Electro-Fenton technology for wastewater treatment: A bibliometric analysis of current research trends, future perspectives and energy consumption analysis. *J. Water Process Eng.* **2021**, *40*, 101952. [CrossRef]
24. Zhang, Z.; Meng, H.; Wang, Y.; Shi, L.; Wang, X.; Chai, S. Fabrication of graphene@graphite-based gas diffusion electrode for improving H_2O_2 generation in Electro-Fenton process. *Electrochim. Acta* **2018**, *260*, 112–120. [CrossRef]
25. Yang, W.; Zhou, M.; Oturan, N.; Li, Y.; Oturan, M.A. Electrocatalytic destruction of pharmaceutical imatinib by electro-Fenton process with graphene-based cathode. *Electrochim. Acta* **2019**, *305*, 285–294. [CrossRef]
26. Orimolade, B.O.; Zwane, B.N.; Koiki, B.A.; Rivallin, M.; Bechelany, M.; Mabuba, N.; Lesage, G.; Cretin, M.; Arotiba, O.A. Coupling cathodic electro-fenton with anodic photo-electrochemical oxidation: A feasibility study on the mineralization of paracetamol. *J. Environ. Chem. Eng.* **2020**, *8*, 104394. [CrossRef]
27. Guo, W.; Zhao, Q.; Du, J.; Wang, H.; Li, X.; Ren, N. Enhanced removal of sulfadiazine by sulfidated ZVI activated persulfate process: Performance, mechanisms and degradation pathways. *Chem. Eng. J.* **2020**, *388*, 124303. [CrossRef]
28. Li, W.; Zhang, Y.; Zhao, P.; Zhou, P.; Liu, Y.; Cheng, X.; Wang, J.; Yang, B.; Guo, H. Enhanced kinetic performance of peroxymonosulfate/ZVI system with the addition of copper ions: Reactivity, mechanism, and degradation pathways. *J. Hazard. Mater.* **2020**, *393*, 122399. [CrossRef]
29. Fu, S.; Jia, H.; Meng, X.; Guo, Z.; Wang, J. Fe-C micro-electrolysis-electrocoagulation based on BFDA in the pre-treatment of landfill leachate: Enhanced mechanism and electrode decay monitoring. *Sci. Total Environ.* **2021**, *781*, 146797. [CrossRef]
30. Chen, R.-F.; Wu, L.; Zhong, H.-T.; Liu, C.-X.; Qiao, W.; Wei, C.-H. Evaluation of electrocoagulation process for high-strength swine wastewater pretreatment. *Sep. Purif. Technol.* **2021**, *272*, 118900. [CrossRef]
31. Sánchez, M.; Gonzalo, O.G.; Yáñez, S.; Ruiz, I.; Soto, M. Influence of nutrients and pH on the efficiency of vertical flow constructed wetlands treating winery wastewater. *J. Water Process Eng.* **2021**, *42*, 102103. [CrossRef]
32. Hufschmid, A.; Becker-Van Slooten, K.; Strawczynski, A.; Vioget, P.; Parra, S.; Péringer, P.; Pulgarin, C. BOD_5 measurements of water presenting inhibitory Cu^{2+}.: Implications in using of BOD to evaluate biodegradability of industrial wastewaters. *Chemosphere* **2003**, *50*, 171–176. [CrossRef]
33. Rachidi, L.; Kaichouh, G.; Khachani, M.; Zarrouk, A.; El Karbane, M.; Chakchak, H.; Warad, I.; EL Hourch, A.; El Kacemi, K.; Guessous, A. Optimization and modeling of the electro-Fenton process for treatment of sertraline hydrochloride: Mineralization efficiency, energy cost and biodegradability enhancement. *Chem. Data Collect.* **2021**, *35*, 100764. [CrossRef]
34. García-Espinoza, J.D.; Robles, I.; Durán-Moreno, A.; Godínez, L.A. Study of simultaneous electro-Fenton and adsorption processes in a reactor containing porous carbon electrodes and particulate activated carbon. *J. Electroanal. Chem.* **2021**, *895*, 115476. [CrossRef]
35. Radjenovic, J.; Bagastyo, A.; Rozendal, R.A.; Mu, Y.; Keller, J.; Rabaey, K. Electrochemical oxidation of trace organic contaminants in reverse osmosis concentrate using RuO_2/IrO_2-coated titanium anodes. *Water Res.* **2011**, *45*, 1579–1586. [CrossRef]
36. Santos, M.J.R.; Medeiros, M.C.; Oliveira, T.M.B.F.; Morais, C.C.O.; Mazzetto, S.E.; Martínez-Huitle, C.A.; Castro, S.S.L. Electrooxidation of cardanol on mixed metal oxide (RuO_2-TiO_2 and IrO_2-RuO_2-TiO_2) coated titanium anodes: Insights into recalcitrant phenolic compounds. *Electrochim. Acta* **2016**, *212*, 95–101. [CrossRef]
37. Estrada, A.L.; Li, Y.-Y.; Wang, A. Biodegradability enhancement of wastewater containing cefalexin by means of the electro-Fenton oxidation process. *J. Hazard. Mater.* **2012**, *227–228*, 41–48. [CrossRef]
38. Deng, F.; Olvera-Vargas, H.; Garcia-Rodriguez, O.; Qiu, S.; Ma, F.; Chen, Z.; Lefebvre, O. Unconventional electro-Fenton process operating at a wide pH range with Ni foam cathode and tripolyphosphate electrolyte. *J. Hazard. Mater.* **2020**, *396*, 122641. [CrossRef]
39. Brillas, E.; Sirés, I.; Oturan, M.A. Electro-Fenton process and related electrochemical technologies based on Fenton's reaction chemistry. *Chem. Rev.* **2009**, *109*, 6570–6631. [CrossRef]
40. Zheng, Y.; Qiu, S.; Deng, F.; Zhu, Y.; Li, G.; Ma, F. Three-dimensional electro-Fenton system with iron foam as particle electrode for folic acid wastewater pretreatment. *Sep. Purif. Technol.* **2019**, *224*, 463–474. [CrossRef]
41. Huo, S.; Necas, D.; Zhu, F.; Chen, D.; An, J.; Zhou, N.; Liu, W.; Wang, L.; Cheng, Y.; Liu, Y.; et al. Anaerobic digestion wastewater decolorization by H_2O_2-enhanced electro-Fenton coagulation following nutrients recovery via acid tolerant and protein-rich Chlorella production. *Chem. Eng. J.* **2021**, *406*, 127160. [CrossRef]

42. Dindaş, G.B.; Çalışkan, Y.; Çelebi, E.E.; Tekbaş, M.; Bektaş, N.; Yatmaz, H.C. Treatment of pharmaceutical wastewater by combination of electrocoagulation, electro-fenton and photocatalytic oxidation processes. *J. Environ. Chem. Eng.* **2020**, *8*, 103777. [CrossRef]
43. Senthilnathan, J.; Younis, S.A.; Kwon, E.E.; Surenjana, A.; Kimb, K.-H.; Yoshimurae, M. An efficient system for electro-Fenton oxidation of pesticide by a reduced graphene oxide-aminopyrazine@3DNi foam gas diffusion electrode. *J. Hazard. Mater.* **2020**, *400*, 123323. [CrossRef] [PubMed]
44. Ren, G.; Zhou, M.; Zhang, Q.; Xu, X.; Li, Y.; Su, P. A novel stacked flow-through electro-Fenton reactor as decentralized system for the simultaneous removal of pollutants (COD, NH_3-N and TP) and disinfection from domestic sewage containing chloride ions. *Chem. Eng. J.* **2020**, *387*, 124037. [CrossRef]
45. McQuillan, R.V.; Stevens, G.W.; Mumford, K.A. Assessment of the electro-Fenton pathway for the removal of naphthalene from contaminated waters in remote regions. *Sci. Total Environ.* **2021**, *762*, 143155. [CrossRef]
46. Midassi, S.; Bedoui, A.; Bensalah, N. Efficient degradation of chloroquine drug by electro-Fenton oxidation: Effects of operating conditions and degradation mechanism. *Chemosphere* **2020**, *260*, 127558. [CrossRef]
47. Lacasa, E.; Cañizares, P.; Llanos, J.; Rodrigo, M.A. Removal of nitrates by electrolysis in non-chloride media: Effect of the anode material. *Sep. Purif. Technol.* **2011**, *80*, 592–599. [CrossRef]
48. Wang, D.; Hu, J.; Liu, B.; Hou, H.; Yang, J.; Li, Y.; Zhu, Y.; Liang, S.; Xiao, K. Degradation of refractory organics in dual-cathode electro-Fenton using air-cathode for H_2O_2 electrogeneration and microbial fuel cell cathode for Fe^{2+} regeneration. *J. Hazard. Mater.* **2021**, *412*, 125269. [CrossRef]
49. Zhang, J.; Qiu, S.; Feng, H.; Hu, T.; Wu, Y.; Luo, T.; Tang, W.; Wang, D. Efficient degradation of tetracycline using core–shell Fe@Fe_2O_3-CeO_2 composite as novel heterogeneous electro-Fenton catalyst. *Chem. Eng. J.* **2022**, *428*, 131403. [CrossRef]
50. Barhoumi, N.; Olvera-Vargas, H.; Oturan, N.; Huguenot, D.; Gadri, A.; Ammar, S.; Brillas, E.; Oturan, M.A. Kinetics of oxidative degradation/mineralization pathways of the antibiotic tetracycline by the novel heterogeneous electro-Fenton process with solid catalyst chalcopyrite. *Appl. Catal. B Environ.* **2017**, *209*, 637–647. [CrossRef]
51. Zhang, Y.; Zuo, S.; Zhou, M.; Liang, L.; Ren, G. Removal of tetracycline by coupling of flow-through electro-Fenton and in-situ regenerative active carbon felt adsorption. *Chem. Eng. J.* **2018**, *335*, 685–692. [CrossRef]
52. Luo, T.; Feng, H.; Tang, L.; Lu, Y.; Tang, W.; Chen, S.; Yu, J.; Xie, Q.; Ouyang, X.; Chen, Z. Efficient degradation of tetracycline by heterogeneous electro-Fenton process using Cu-doped Fe@Fe_2O_3: Mechanism and degradation pathway. *Chem. Eng. J.* **2020**, *382*, 122970. [CrossRef]
53. Zwane, B.N.; Orimolade, B.O.; Koiki, B.A.; Mabuba, N.; Gomri, C.; Petit, E.; Bonniol, V.; Lesage, G.; Rivallin, M.; Cretin, M.; et al. Combined Electro-Fenton and Anodic Oxidation Processes at a Sub-Stoichiometric Titanium Oxide (Ti_4O_7) Ceramic Electrode for the Degradation of Tetracycline in Water. *Water* **2021**, *13*, 2772. [CrossRef]
54. Olvera-Vargas, H.; Gore-Datar, N.; Garcia-Rodriguez, O.; Mutnuri, S.; Lefebvre, O. Electro-Fenton treatment of real pharmaceutical wastewater paired with a BDD anode: Reaction mechanisms and respective contribution of homogeneous and heterogeneous OH. *Chem. Eng. J.* **2021**, *404*, 126524. [CrossRef]
55. Feng, Y.; Yang, S.; Xia, L.; Wang, Z.; Suo, N.; Chen, H.; Long, Y.; Zhou, B.; Yu, Y. In-situ ion exchange electrocatalysis biological coupling (i-IEEBC) for simultaneously enhanced degradation of organic pollutants and heavy metals in electroplating wastewater. *J. Hazard. Mater.* **2019**, *364*, 562–570. [CrossRef] [PubMed]
56. Salles, N.A.; Fourcade, F.; Geneste, F.; Floner, D.; Amrane, A. Relevance of an electrochemical process prior to a biological treatment for the removal of an organophosphorous pesticide, phosmet. *J. Hazard. Mater.* **2010**, *181*, 617–623. [CrossRef]
57. Yao, B.; Luo, Z.; Yang, J.; Zhi, D.; Zhou, Y. FeIIFeIII layered double hydroxide modified carbon felt cathode for removal of ciprofloxacin in electro-Fenton process. *Environ. Res.* **2021**, *197*, 111144. [CrossRef]
58. Johnson, M.B.; Mehrvar, M. Treatment of Actual Winery Wastewater by Fenton-like Process: Optimization to Improve Organic Removal, Reduce Inorganic Sludge Production and Enhance Co-Treatment at Municipal Wastewater Treatment Facilities. *Water* **2021**, *14*, 39. [CrossRef]
59. Dung, N.T.; Duong, L.T.; Hoa, N.T.; Thao, V.D.; Ngan, L.V.; Huy, N.N. A comprehensive study on the heterogeneous electro-Fenton degradation of tartrazine in water using $CoFe_2O_4$/carbon felt cathode. *Chemosphere* **2022**, *287*, 132141. [CrossRef]
60. Ma, B.; Lv, W.; Li, J.; Yang, C.; Tang, Q.; Wang, D. Promotion removal of aniline with electro-Fenton processes utilizing carbon nanotube 3D morphology modification of an Ag-loaded copper foam cathode. *J. Water Process Eng.* **2021**, *43*, 102295. [CrossRef]
61. Thor, S.-H.; Ho, L.-N.; Ong, S.-A.; Abidin, C.Z.A.; Heah, C.-Y.; Nordin, N.; Ong, Y.-P.; Yap, K.-L. Advanced oxidation treatment of amaranth dye synchronized with electricity generation using carbon-based cathodes in a sustainable photocatalytic fuel cell integrated electro-fenton system. *J. Environ. Chem. Eng.* **2021**, *9*, 106439. [CrossRef]
62. Dong, P.; Liu, W.; Wang, S.; Wang, H.; Wang, Y.; Zhao, C. In suit synthesis of Fe_3O_4 on carbon fiber paper@polyaniline substrate as novel self-supported electrode for heterogeneous electro-Fenton oxidation. *Electrochim. Acta* **2019**, *308*, 54–63. [CrossRef]
63. Deng, J.; Lu, J.; Yan, Q.; Pan, J. Basic research on chemical mechanical polishing of single-crystal SiC—Electro–Fenton: Reaction mechanism and modelling of hydroxyl radical generation using condition response modelling. *J. Environ. Chem. Eng.* **2021**, *9*, 104954. [CrossRef]
64. Sun, M.; Zhang, Z.; Liu, G.; Lv, M.; Feng, Y. Enhancing methane production of synthetic brewery water with granular activated carbon modified with nanoscale zero-valent iron (NZVI) in anaerobic system. *Sci. Total Environ.* **2021**, *760*, 143933. [CrossRef]

65. Wang, J.; Chen, R.; Fan, L.; Cui, L.; Zhang, Y.; Cheng, J.; Wu, X.; Zeng, W.; Tian, Q.; Shen, L. Construction of fungi-microalgae symbiotic system and adsorption study of heavy metal ions. *Sep. Purif. Technol.* **2021**, *268*, 118689. [CrossRef]
66. Zhang, A.; Wang, S.; Yang, M.; Li, H.; Wang, H.; Fang, F.; Guo, J. Influence of NaCl salinity on the aggregation performance of anammox granules. *J. Water Process Eng.* **2020**, *39*, 101687. [CrossRef]
67. Sun, D.; Hong, X.; Cui, Z.; Du, Y.; Hui, K.S.; Zhu, E.; Wu, K.; Hui, K.N. Treatment of landfill leachate using magnetically attracted zero-valent iron powder electrode in an electric field. *J. Hazard. Mater.* **2020**, *388*, 121768. [CrossRef]
68. Chu, Y.; Miao, B.; Zhang, X.; Lv, R. Heterogeneous electro-Fenton-like oxidation for the degradation of 4-nitrophenol characterized by immobilized Fe(III): Performance, mechanism and chlorinated organic compounds formation. *J. Water Process Eng.* **2020**, *38*, 101662. [CrossRef]
69. Kaspar, P.; Sobola, D.; Dallaev, R.; Ramazanov, S.; Nebojsa, A.; Rezaee, S.; Grmela, L. Characterization of Fe_2O_3 thin film on highly oriented pyrolytic graphite by AFM, Ellipsometry and XPS. *Appl. Surf. Sci.* **2019**, *493*, 673–678. [CrossRef]
70. Liang, J.; Xiang, Q.; Lei, W.; Zhang, Y.; Sun, J.; Zhu, H.; Wang, S. Ferric iron reduction reaction electro-Fenton with gas diffusion device: A novel strategy for improvement of comprehensive efficiency in electro-Fenton. *J. Hazard. Mater.* **2021**, *412*, 125195. [CrossRef]
71. Ye, Z.; Padilla, J.A.; Xuriguera, E.; Brillas, E.; Sirés, I. Magnetic MIL(Fe)-type MOF-derived N-doped nano-ZVI@C rods as heterogeneous catalyst for the electro-Fenton degradation of gemfibrozil in a complex aqueous matrix. *Appl. Catal. B Environ.* **2020**, *266*, 118604. [CrossRef]
72. Wang, R.; Shu, J.; Chen, M.; Wang, R.; He, D.; Wang, J.; Tang, C.; Han, Y.; Luo, Z. An innovative method for fractionally removing high concentrations of Ni^{2+}, PO_4^{3-}, TP, COD, and NH_4^+-N from printed-circuit-board nickel plating wastewater. *Sep. Purif. Technol.* **2021**, *260*, 118241. [CrossRef]
73. Kumar, N.; Sreenivasa, S.; Prashant, A.; Kumar, V.; Holla, B.S.; Chandramohan, V.; Vishwantha, P.; Yadav, A.K. N′-((3-(substituted phenyl)-1-phenyl-1H-Pyrazol-4-yl)methylene)-(substituted) benzhydrazide: Synthesis, characterization and pharmacological evaluation. *Chem. Data Collect.* **2021**, *32*, 100665. [CrossRef]
74. Mojsiewicz-Pieńkowska, K. Size exclusion chromatography with evaporative light scattering detection as a method for speciation analysis of polydimethylsiloxanes. III. Identification and determination of dimeticone and simeticone in pharmaceutical formulations. *J. Pharm. Biomed. Anal.* **2012**, *58*, 200–207. [CrossRef]
75. Yang, X.; Sun, Z.; Wang, W.; Zhou, Q.; Shi, G.; Wei, F.; Jiang, G. Developmental toxicity of synthetic phenolic antioxidants to the early life stage of zebrafish. *Sci. Total Environ.* **2018**, *643*, 559–568. [CrossRef]
76. Wang, W.; Xiong, P.; Zhang, H.; Zhu, Q.; Liao, C.; Jiang, G. Analysis, occurrence, toxicity and environmental health risks of synthetic phenolic antioxidants: A review. *Environ. Res.* **2021**, *201*, 111531. [CrossRef]
77. Zhang, X.; Lu, X.; Li, H. Isolation and identification of a novel allelochemical from Ruppia maritima extract against the cyanobacteria Microcystis aeruginosa. *Environ. Technol. Innov.* **2021**, *21*, 101301. [CrossRef]
78. Seibert, D.; Borba, F.H.; Bueno, F.; Inticher, J.J.; Módenes, A.N.; Espinoza-Quiñones, F.R.; Bergamasco, R. Two-stage integrated system photo-electro-Fenton and biological oxidation process assessment of sanitary landfill leachate treatment: An intermediate products study. *Chem. Eng. J.* **2019**, *372*, 471–482. [CrossRef]